

Electrical Analysis of Minocycline Eluting Layer-By-Layer Thin-Films from Functional Micro-Electrode Arrays

Matthew D. McDermott*, *IEEE Student Member*, Kaitlynn P. Olczak*, *IEEE Student Member*, and Kevin J. Otto, *IEEE Member*.

Abstract— Although the potential for intracortical implanted microelectrodes has been demonstrated, successful clinical translation has been hindered by their inability to function over clinically relevant time-points (years to decades). Failure of implanted microelectrode arrays (MEA's) has been highly correlated with the foreign body response which progressively encapsulates the MEA's in a glial sheath, isolating them from the surrounding microenvironment. To mitigate this response, drug delivery has been implemented to release therapeutics from the device surface. This has allowed limited success at acute time points; however, challenges in maintaining long-term therapeutic dosages has resulted in an inability to mitigate chronic inflammation. A recent publication has demonstrated the use of multi-layer film composed of dextran-sulfate, minocycline hydrochloride (MH), and gelatin type A, assembled via layer-by-layer technology, capable of providing sustained release of MH for several weeks; however, their impact on functionality has not yet been analyzed. We found that after being coated with 20 layers NeuroNexus devices exhibited significantly increased impedance at 100Hz, 1kHz, and 10kHz, though this was significantly reduced after 24-hours of incubation in PBS. Charge carrying capacity also significantly increased after incubation in PBS. It can be concluded that these coatings do influence MEA's immediately after coating, but is less impactful over time as the coating degrades.

I. INTRODUCTION

Neural interfacing (NI) devices are used in current and emerging functional restoration applications. The invasiveness of a device being directly correlated with functional selectivity of the device itself [1], [2]. The cochlear implant is an example of a NI device that has demonstrated its clinical value, with nearly 220,000 implanted individuals worldwide in 2011 [3]. Beyond

This work was sponsored by Defense Advanced Research Projects Agency (DARPA) Microsystems Technology Office (MTO), under the auspices of Dr. Jack W. Judy and Dr. Douglas Weber Pacific Grant No. N66001-11-1-4013 and by the University of Florida Preeminent Initiative Start-up Funds.

*Matthew McDermott and Kaitlynn Olczak contributed equally to this research and the writing of the manuscript.

Matthew D McDermott is with the Weldon School of Biomedical Engineering, Purdue University, West Lafayette, IN 47907 USA, and the J Pruitt Family of Biomedical Engineering, University of Florida, Gainesville, FL 32611 USA, (e-mail: m.mcdermott1984@ufl.edu).

Kaitlynn P Olczak, is with the J Pruitt Family of Biomedical Engineering, University of Florida, Gainesville, FL 32611 USA, (e-mail: kpolczak@ufl.edu).

Kevin J Otto is with the J Pruitt Family of Biomedical Engineering, University of Florida, Gainesville, FL 32611 USA, (phone: 352-294-2227; fax: 352-273-9221; e-mail: kevin.otto@bme.ufl.edu).

somatosensory restoration, NI devices have been employed in treatments for Parkinson's disease [4] as well as motor control of prosthetic limbs [5]. The potential for MEA's has been demonstrated with the use of implanted NI's to give tetraplegic individuals the ability to control a robotic arm, with three-dimensional reach and grasp function [5]. However, successful clinical translation has been hindered by the inability of MEA's to function with high reliability at clinically relevant time scales (years to decades) [6]. Device failure has been attributed to the accumulation of both mechanical and biological mechanisms. Mechanical failures include material failures of the device such as cracking of the electrical traces [7] and delamination [8]. Biological failure encompasses the tissues reaction to the insertion and sustained presence of the device, and is characterized by a multiphase Foreign Body Response (FBR) [9]–[11].

Disruption of the Blood Brain Barrier (BBB) consequent to implantation allows for the penetration of blood born macrophage and sera, into neural tissue [12]. Microglia in the surrounding tissue are immediately activated and begin to move processes towards the implanted device within 30 minutes [13]. Within 24-hours after implantation, activated microglia encapsulate the device and astrocytes begin activation [9]. By one week, astrocytes are fully activated; by week two, they have formed a compact sheath surrounding the device [9], [10], [14]. This glial sheath is thought to effectively isolate the MEA from the surrounding tissue, as tight junctions between the glia cells obstruct ion diffusion [15], and the cells membranes themselves increase impedance [16]–[18]. In addition to acting as an electrical barrier, the glial sheath acts as a physical barrier, increasing the distance between the device and surrounding neurons. This increased distance effects both recording and stimulating performance by decreasing neuronal signal amplitude [21], and increasing stimulation thresholds [1].

Attempts to mitigate inflammation have involved modifications to device architecture [21], stiffness [22], [23] and surface modification [24], [25]. Therapeutic interventions have also been implemented via systemic delivery [26] direct adherence to the device [27], or drug elution via coatings on the device surface [28], [29]; while these strategies have shown limited success at acute time points, limited release duration has prevented significant changes at chronic time-points. Attaining long-term release of therapeutic concentrations is one challenge limiting success at chronic time points and is restricted by a need to minimize total device thickness. Minimizing coating thickness is essential with regard to causing negligible increases to the device

footprint, as large footprints generate greater tissue strain and have been demonstrated to increase FBR severity [30]. Perhaps the most important consideration is the coatings impact on the devices' electrical properties, namely impedance and charge carrying capacity. Low impedance electrodes are needed for high resolution recording and stimulation, as increased impedance reduces signal-to-noise ratio and increases the applied potential, which could potentially induce tissue damage [31]. Recently the Zhong lab demonstrated a variety of Layer-By-Layer (LBL) strategies, which allowed for the release of several relevant anti-inflammatory moieties including minocycline hydrochloride [32] and neurotrophin [33], showing the controlled release of the agents for weeks while increasing the coated surface by mere microns. However, the impact of these coatings on an MEA is currently unknown. Without understanding the impact of the coatings on MEA impedance and Charge Carrying Capacity (CCC), the implementation of LBL strategies upon MEA devices *in vivo* is unwise. In this study, we explore the impact of a 20 tri-layer minocycline hydrochloride loaded LBL coating upon functional NeuroNexus MEA's to assess the electrical impedance and CCC, before coating, after coating and 24-hours post drug release incubation.

II. MATERIALS AND METHODS

All LBL procedures were adapted from previous literature established in the field [32], [33].

A. Wafer Dicing and Cleaning

Four-inch p-type silicon wafers (Silicon Quest International, San Jose, CA 95134) were cut to size, 4.5x13 mm, then marked for holding placement (0.3 mm below top) to generate 4.5 x 10 mm area for coating using an ADT 7100 Dicing Saw (ADT, Yokneam, Israel). Newly diced wafers were then submerged in a piranha solution to remove organic contaminants, 1:1 hydrogen peroxide (30%w/v.)

B. LBL Solution Preparation

Stock solutions of Minocycline Hydrochloride (MH) (Sigma-Aldrich, St. Louis, MO), gelatin type A, 300 bloom (Sigma-Aldrich, St. Louis, MO), and polyethylenimine, MW 25kD (Polysciences Inc., Warminster PA) were all prepared in DDi water at 1% w/v while dextran sulfate (Sigma-Aldrich, St. Louis, MO), was prepared at 1mg/ml in 14.4 mM MgCl₂ in Double Deionized (DDi) water.

B. LBL Coating Procedure

An automated dip-coater (Gilson, Middletown, WI) was used for the LBL coating procedure. The wafers were first submerged in PEI solution for ten minutes, followed by a one minute wash in DDi water, to form an initial positive base layer. The tri-layer was formed by dipping the wafer into the GA, MH then DS-Mg solutions, with a 1 minute DDi water rinse following submersion in each solution. The tri-layer coating procedure was repeated until 20 tri-layers were obtained and allowed to air dry upon completion.

Coatings on the MEA's were performed following the same procedure, with devices being submerged to a depth ensuring complete coating of the silicon shank.

D. Coating Thickness Analysis

A profilometer (Tencor AS500, Milpitas, CA) was used for all coating thickness measurements (n=3). Coated wafers were scored with a razor to remove a section of the coating at the bottom of the chip. The displacement from the silicon wafer and the coating was then measured at 3 points.

E. In Vitro Release and Analysis of Minocycline

Coated wafers (n=3) were placed in 500 μ L 1X PBS, shielded from light exposure, and placed on a rocker at 200 RPM at 37°C. PBS was removed at 24-hour intervals and replaced with pre-warmed PBS. Minocycline concentrations were quantified using a spectrophotometer (BioTek, Winooski, VT) at 350 nm.

F. Electrical Set-up and Analysis

Three, Type-A, 16 channel, single shank MEA's (NeuroNexus, Ann Arbor, MI) with electrode surface area of 703 μ m² were used for electrical analysis. Devices were measured prior to coating, immediately after coating, and 24-hours after incubating in PBS at 37°C. Using a three-electrode set-up, the NeuroNexus electrode functioned as the working electrode, and a calomel electrode (Fisher Scientific, Hampton, NH) and platinum wire as the reference and counter electrodes respectively. All measurements were made with an Autolab potentiostat PGSTAT12 (EcoChemie, Utrecht, The Netherlands) with built in frequency analyzer (Brinkman, Westbury, NY). Measurements from each electrode site were compared to the sites pre-coated value for percent change calculations.

Electrochemical Impedance Spectroscopy (EIS) was used to obtain impedance measurements. A 10mV sine wave (wave type=15 sines) was applied to electrode sites at frequencies ranging logarithmically from 10Hz to 30kHz.

Cyclic Voltammetry was performed by sweeping the voltage linearly from -0.6 to 0.8 V at a scanning rate of 0.5V/s. CCC was calculated by integrating the cyclic voltammogram's cathodic current density curve and dividing by the sweep rate.

F. Statistics

A two-tailed, single sample t-test was used to compare measured thickness to reported values. Multiple group comparisons for EIS analysis were performed using a Friedman ANOVA, followed by nonparametric multiple comparisons with adjusted α . Nonparametric analysis were selected due to non-normality of the distributions. All values shown as mean \pm standard mean error, for all tests significance was indicated at $\alpha < .05$.

III. RESULTS AND DISCUSSION

Prior to understanding the impact of the LBL coatings on the MEA's, it was necessary to confirm the reproduction of previous findings. As such, we analyzed both the drug

release performance and coating thickness as a means of verifying reproduction of the previous LBL work.

A. Demonstration of Reproducibility

Verification of the LBL coatings was first assessed through comparison of coating thicknesses. The 20 tri-layer coatings had an average thickness of $1.6 \pm 0.5 \mu\text{m}$, resulting in an average thickness of $80 \pm 20 \text{nm}$ per tri-layer (Fig. 1A). This was not significantly different than the expected 62.5nm per tri-layer thickness previously reported. To further validate the reproduction of coating features we then evaluated minocycline release *in vitro* (Fig. 1B). Similar release trends were observed, although inherent detection limits prohibited quantifiable measurements after the fifth day of release. Low minocycline concentrations can be attributed to the small surface area of the wafers, 0.45cm^2 , chosen in the interest of emulating any potential variations in coating characteristics due to significant surface area reductions (i.e. edge effects), while maintaining a reasonable extent of release detection.

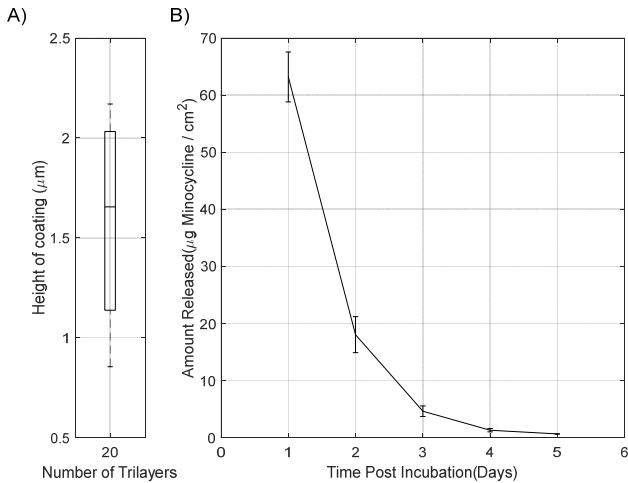


Figure 1. Coating thickness and drug release for verification of coating properties. A) Visualization of the thickness of a 20 LBL coating paradigm on a silicon wafer. B) The drug release from the chips *in vitro* exhibit a similar release profile to that as previously described in literature.

B. Characterization of Electrical Properties

Upon verification of successful reproduction of the LBL coatings, the effect of the coatings on the electrical properties of MEA's were evaluated. Uncoated EIS measurements were compared to measurements taken after coating and 24-hours incubation, to ascertain the coatings' initial and dynamic effects on electrical characteristics. Coatings were found to have minimal effect on the average CCC, albeit the reduced variance in post-coating CCC resulted in the values showing a significant difference between the pre- and post-coated averages (Fig. 2A). CCC 24-hours after incubation in PBS was found to be significantly different than both the pre- and post-coating CCC. We hypothesize that this increase in CCC was likely due the hydration of the gelatin and Mg^{2+} ions within the LBL coatings which allow increased current flow resulting in the increased CCC.

The impedance increased at all observed frequencies post-coating (Fig. 2B), however this increase was shown to be reduced after just 24-hours incubation in PBS at 37°C . The impedance continued to decrease throughout experiment. We hypothesize that this was likely due to coating degradation as minocycline, gelatin, Mg^{2+} , and dextran sulfate elute away.

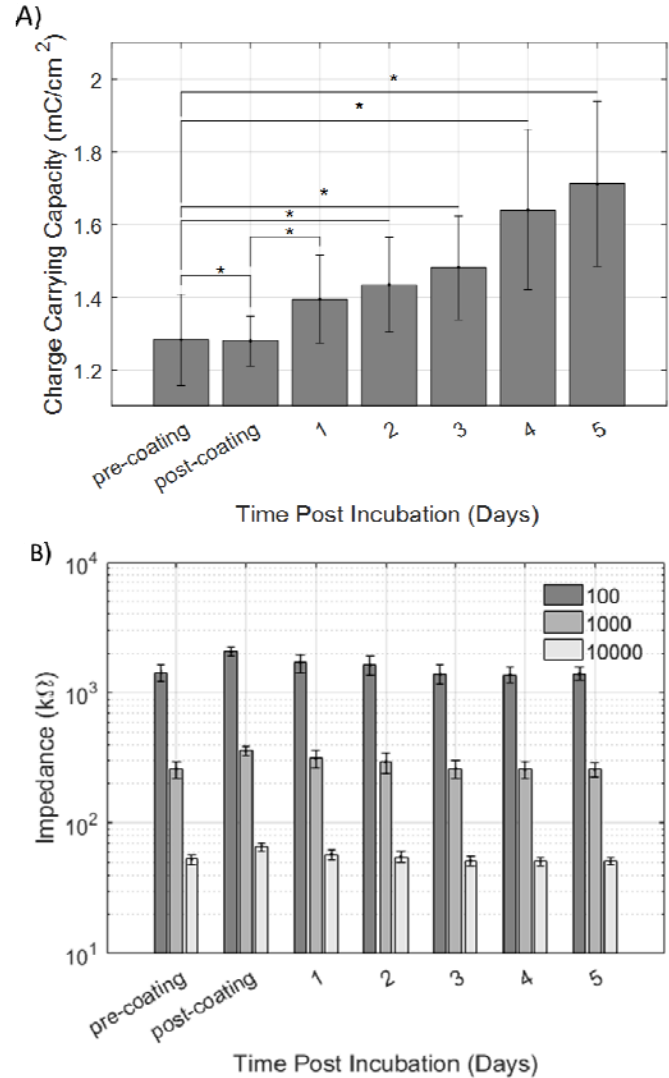


Figure 2. CCC and EIS measurements pre-coating, post-coating, and five days post incubation. A) CCC is initially unchanged after being coated, though increases over the incubation period. B) EIS is initially increased after devices are coated; however, this increase is reduced 1-day post incubation, though significantly higher than pre-coated impedance. Data shown as mean \pm SEM

IV. CONCLUSION

Previous research has shown the potential for LBL systems to deliver therapeutic doses of minocycline from an MEA device for weeks at a time; however, the impact of these coatings on device performance was previously unknown. Although it was shown that at these coatings do increase CCC and impedance after coating, our results indicate that these increases are only temporary and the benefits of the system outweigh the impact on device performance. However, it would be prudent to extend the

study to analyze the impact of the coatings on MEA devices for a longer duration and with other coating paradigms.

ACKNOWLEDGMENT

The authors wish to thank all current and former members of the NPR Lab and the UF BME IT Department. This work was sponsored by Defense Advanced Research Projects Agency (DARPA) Microsystems Technology Office (MTO), under the auspices of Dr. Jack W. Judy and Dr. Douglas Weber Pacific Grant No. N66001-11-1-4013 and by the University of Florida Pre-eminent Initiative Start-up Funds.

REFERENCES

- [1] R. V. Shannon, J. K. Moore, D. B. McCreery, and F. Portillo, "Threshold-distance measures from electrical stimulation of human brainstem," *IEEE Trans. Rehabil. Eng.*, vol. 5, no. 1, pp. 70–74, 1997.
- [2] S. D. Stoney, W. D. Thompson, and H. Asanuma, "Excitation of pyramidal tract cells by intracortical microstimulation: effective extent of stimulating current.," *J. Neurophysiol.*, vol. 31, no. 5, pp. 659–669, 1968.
- [3] M. K. Cose, S. B. Waltzman, E. Review, and D. May, "Cochlear implants : current status and future poten al .," *Expert Rev. Med. Devices*, vol. 8, no. 3, 2011.
- [4] C. Universitaria, "Deep-Brain Stimulation of the Subthalamic Nucleus or the Pars," *English J.*, vol. 345, no. 13, pp. 956–963, 2001.
- [5] L. R. Hochberg, D. Bacher, B. Jarosiewicz, N. Y. Masse, D. John, J. Vogel, S. Haddadin, J. Liu, S. S. Cash, J. P. Donoghue, D. Service, and G. Hospital, "Reach and grasp by people with tetraplegia using a neurally controlled robotic arm," *Nature*, vol. 485, no. 7398, pp. 372–375, 2013.
- [6] J. C. Barrese, N. Rao, K. Paroo, C. Triebwasser, C. Vargas-Irwin, L. Franquemont, and J. P. Donoghue, "Failure mode analysis of silicon-based intracortical microelectrode arrays in non-human primates.," *J. Neural Eng.*, vol. 10, no. 6, p. 66014, 2013.
- [7] T. D. Y. Kozai, K. Catt, X. Li, Z. V. Gugel, V. T. Olafsson, A. L. Vazquez, and X. T. Cui, "Mechanical failure modes of chronically implanted planar silicon-based neural probes for laminar recording," *Biomaterials*, vol. 37, pp. 25–39, 2015.
- [8] E. M. Schmidt, J. S. McIntosh, and M. J. Bak, "Long-term implants of Parylene-C coated microelectrodes.," *Med. Biol. Eng. Comput.*, vol. 26, no. 1, pp. 96–101, 1988.
- [9] D. H. Szarowski, M. D. Andersen, S. Retterer, a J. Spence, M. Isaacson, H. G. Craighead, J. N. Turner, and W. Shain, "Brain responses to micro-machined silicon devices.," *Brain Res.*, vol. 983, no. 1–2, pp. 23–35, 2003.
- [10] J. N. Turner, W. Shain, D. H. Szarowski, M. Andersen, S. Martins, M. Isaacson, and H. Craighead, "Cerebral astrocyte response to micromachined silicon implants.," *Exp. Neurol.*, vol. 156, no. 1, pp. 33–49, 1999.
- [11] V. S. Polikov, M. L. Block, J. M. Fellous, J. S. Hong, and W. M. Reichert, "In vitro model of glial scarring around neuroelectrodes chronically implanted in the CNS," *Biomaterials*, vol. 27, no. 31, pp. 5368–5376, 2006.
- [12] T. Saxena, L. Karumbaiah, E. a Gaupp, R. Patkar, K. Patil, M. Betancur, G. B. Stanley, and R. V Bellamkonda, "The impact of chronic blood-brain barrier breach on intracortical electrode function.," *Biomaterials*, vol. 34, no. 20, pp. 4703–13, Jul. 2013.
- [13] T. D. Y. Kozai, A. L. Vazquez, C. L. Weaver, S.-G. Kim, and X. T. Cui, "In vivo two-photon microscopy reveals immediate microglial reaction to implantation of microelectrode through extension of processes.," *J. Neural Eng.*, vol. 9, no. 6, p. 66001, Dec. 2012.
- [14] K. A. Potter, A. C. Buck, W. K. Self, and J. R. Capadona, "Stab injury and device implantation within the brain results in inversely multiphasic neuroinflammatory and neurodegenerative responses," *J. Neural Eng.*, vol. 9, no. 4, p. 46020, 2012.
- [15] T. Roitbak and E. Syková, "Diffusion barriers evoked in the rat cortex by reactive astrogliosis," *Glia*, vol. 28, no. 1, pp. 40–48, 1999.
- [16] W. M. Grill and J. Thomas Mortimer, "Electrical properties of implant encapsulation tissue," *Ann. Biomed. Eng.*, vol. 22, no. 1, pp. 23–33, 1994.
- [17] J. C. Williams, J. A. Hippensteel, J. Dilgen, W. Shain, and D. R. Kipke, "Complex impedance spectroscopy for monitoring tissue responses to inserted neural implants.," *J. Neural Eng.*, vol. 4, no. 4, pp. 410–23, Dec. 2007.
- [18] Otto, Kevin J, M. D. Johnson, and D. R. Kipke, "Voltage pulses change neural interface properties and improve unit recordings with chronically implanted microelectrodes," *IEEE Trans. Biomed. Eng.*, vol. 53, no. 2, pp. 333–340, 2006.
- [19] L. A. Geddes and R. Roeder, "Criteria for the selection of materials for implanted electrodes," *Ann. Biomed. Eng.*, vol. 31, no. 7, pp. 879–890, 2003.
- [20] M. A. Moffitt and C. C. McIntyre, "Model-based analysis of cortical recording with silicon microelectrodes," *Clin. Neurophysiol.*, vol. 116, no. 9, pp. 2240–2250, 2005.
- [21] J. P. Seymour and D. R. Kipke, "Neural probe design for reduced tissue encapsulation in CNS.," *Biomaterials*, vol. 28, no. 25, pp. 3594–607, Sep. 2007.
- [22] S. R. Goldstein and M. Salcman, "Mechanical Factors in the Design of Chronic Recording Intracortical Microelectrodes," *IEEE Trans. Biomed. Eng.*, no. 4, pp. 260–269, 1973.
- [23] Z. Xiang, S.-C. Yen, N. Xue, T. Sun, W. M. Tsang, S. Zhang, L.-D. Liao, N. V<p>Thakor, and C. Lee, "Ultra-thin flexible polyimide neural probe embedded in a dissolvable maltose-coated microneedle," *J. Micromechanics Microengineering*, vol. 24, no. 6, p. 65015, 2014.
- [24] V. S. Polikov, P. a. Tresco, and W. M. Reichert, "Response of brain tissue to chronically implanted neural electrodes," *J. Neurosci. Methods*, vol. 148, pp. 1–18, 2005.
- [25] E. Azemi, C. F. Lagenaur, and X. T. Cui, "The surface immobilization of the neural adhesion molecule L1 on neural probes and its effect on neuronal density and gliosis at the probe/tissue interface.," *Biomaterials*, vol. 32, no. 3, pp. 681–92, Jan. 2011.
- [26] R. L. Rennaker, J. Miller, H. Tang, and D. A. Wilson, "Minocycline increases quality and longevity of chronic neural recordings.," *J. Neural Eng.*, vol. 4, no. 2, pp. L1-5, 2007.
- [27] Y. Zhong and R. V Bellamkonda, "Dexamethasone-coated neural probes elicit attenuated inflammatory response and neuronal loss compared to uncoated neural probes," *Brain Res.*, vol. 1148, no. 1, pp. 15–27, 2007.
- [28] R. Wadhwa, C. F. Lagenaur, and X. T. Cui, "Electrochemically controlled release of dexamethasone from conducting polymer polypyrrole coated electrode," *J. Control. Release*, vol. 110, no. 3, pp. 531–541, 2006.
- [29] M. D. Mcdermott, J. Zhang, and K. J. Otto, "Improving the Brain Machine Interface via Multiple Tetramethyl Orthosilicate Sol-Gel Coatings on Microelectrode Arrays *," vol. 4526, pp. 22–24, 2015.
- [30] S. Sommakia, H. C. Lee, J. Gaire, and K. J. Otto, "Materials approaches for modulating neural tissue responses to implanted microelectrodes through mechanical and biochemical means," *Curr. Opin. Solid State Mater. Sci.*, vol. 18, no. 6, pp. 319–328, Dec. 2014.
- [31] M. R. Abidian and D. C. Martin, "Experimental and theoretical characterization of implantable neural microelectrodes modified with conducting polymer nanotubes," *Biomaterials*, vol. 29, no. 9, pp. 1273–1283, 2008.
- [32] Z. Zhang, J. Nong, and Y. Zhong, "Antibacterial , anti-in fl ammatory and neuroprotective layer-by-layer coatings for neural implants," *J. Neural Eng.*, vol. 12, no. 4, p. 46015.
- [33] Z. Zhang, Q. Li, L. Han, and Y. Zhong, "Layer-by-layer films assembled from natural polymers for sustained release of neurotrophin.," *Biomed. Mater.*, vol. 10, no. 5, p. 55006, 2015.